Polaron in the Wigner lattice

Lenac, Z.; Šunjić, Marijan

Permanent link / Trajna poveznica: https://urn.nsk.hr/urn:nbn:hr:217:825830

Download date / Datum preuzimanja: **2024-04-25**

Repository / Repozitorij:

Repository of the Faculty of Science - University of Zagreb

Polaron in the Wigner lattice

Z. Lenac

Department of Physics, University of Rijeka, 51000 Rijeka, Croatia

M. Šunjić

Department of Physics, University of Zagreb, P.O. Box 162, 10000 Zagreb, Croatia

(Received 21 May 1998; revised manuscript received 28 September 1998)

We analyze the polaron in a Wigner lattice, i.e., the interaction of an external electron with electrons in a quasi-two-dimensional Wigner crystal, configured on a dielectric layer with a metallic substrate. Particular attention is paid to the dynamics of the system and to the electron-phonon interaction. The polaron wave function and ground-state energy of the system are calculated in the extended small-polaron theory. The theory is based on the complete set of Wannier functions, which enables us to treat also the polaron dispersion and the first correction to the standard polaron self-energy. We also discuss the $T=0$ Wigner phase transition, i.e., melting of the electron lattice due to increased electron density. The general agreement with the results obtained previously within the Schrödinger-Rayleigh perturbation theory is good, but also we found some significant differences. The new calculations show that (i) the polaron dispersion is significant at all electron densities and in most cases it resembles the dispersion of lattice electrons; (ii) the critical density parameter r_c for a Wigner phase transition in a high density region is close to the value $r_c \approx 40$ predicted for a strictly two-dimensional Wigner lattice, regardless of the dielectric layer thickness. [S0163-1829(99)02110-4]

I. INTRODUCTION

Electron-phonon interaction is by all means one of the most investigated problems in the solid state physics. Standardly it assumes the interaction of a free-like electron with the vibrations of the atoms (ions) in the crystal lattice. As a result, the electron is ''dressed'' by lattice phonons and recognized as a polaron. Here we are interested in a quasi-two-dimensional (2D) Wigner lattice. This lattice, theoretically predicted long ago by Wigner[1] and first experimentally detected by Grimes and Adams,[2] is formed by electrons on a dielectric layer at very low temperatures. Obviously, one can add an external electron among lattice electrons and ask for the interaction of this free-like electron with lattice vibrations, i.e., for the polaron in the Wigner lattice. While the lattice vibrations are known,[3,4] here we wish to investigate the properties of a Wigner polaron. There are some obvious differences between this and the standard polaron problem. Namely the lattice electrons are much lighter than the atoms so the electron-phonon interaction is expected to be much stronger. Also lattice electrons will try to repel the free-like (external) electron rather than to attract it. In that sense the external electron will ''hop'' from one site in between the lattice electrons to another instead of ''hopping'' from one lattice point to another. There is another possibility for the external electron, i.e., it can become a regular lattice electron. The critical density which divides those two qualitatively different behaviors of the system can be determined and then used as a definition for the $T=0$ Wigner phase transition.[5]

To our knowledge the problem of a polaron in a Wigner lattice was not much investigated. A similar problem was recently analyzed for a bilayer electron system.[6] In that case an electron at a fixed distance from the 2D Wigner lattice interacts with lattice electrons thus forming a ''remote polar-

on.'' In high T_c superconductors one also uses the term ''Wigner polaron.'' But in that case the electrons of Wigner lattice interact with the phonons of superconductor lattice and thus behave as polarons.[7] In our model the lattice electrons are deposited on a dielectric layer with a metallic substrate (which provides charge neutrality) and we take into account only their static interaction with the substrate through the image potential. The dynamical screening occurs when an external electron, added in between the lattice electrons, interacts with lattice phonons and as a main effect shifts them into coherent states.

In Ref. 5, hereafter denoted as I, we have analyzed the polaron in the Wigner lattice within the Schrödinger-Rayleigh perturbation theory, treating electron-phonon interaction as a perturbation. The system was the same as the one discussed here, i.e., quasi-2D Wigner lattice on a dielectric layer with a metallic substrate. Recently (Ref. 8) we tested the theory developed in I in the purely theoretical model of a *strictly* 2D Wigner lattice. Notice that within this model there is no image potential and no difference between the average electron-electron interaction and the screening due to the positive background, which were important in I. We calculated the $T=0$ phase transition of a Wigner lattice and obtained $r_c = 16$, where r_c is the critical, phase-transition value of the density parameter $r_s = 1/\sqrt{\pi n} a_0$. Here a_0 is the Bohr radius and n is the 2D electron concentration. The first-principle ground-state calculations[9] give $r_c = 37 \pm 5$, so we had to reexamine our approach. We found that for a strictly 2D Wigner lattice the electron-phonon interaction is very important and therefore cannot be successfuly treated as a perturbation. We developed a new approach, based on an extended small-polaron theory, which gave us the expected result[8] $r_c \approx 40$.

The above discussion stresses great influence of the dynamical screening of an external electron on the determina-

tion of the $T=0$ Wigner phase transition. Clearly, the dynamical screening is an essential problem *per se* so in this article we elaborate our new approach in more detail than in Ref. 8 and apply it to the more adequate model of a quasi-2D (i.e., perpendicularly delocalized) Wigner lattice on a substrate. Besides the $T=0$ Wigner phase transition, we discuss in particular the polaron localization, self-energy and dispersion and compare it with the dispersion of lattice phonons. We analyze properties of a Wigner polaron following the basic concept of the small-polaron theory,[10] but without making the approximations characteristic for this theory when it deals with an *atomic* lattice. In that sense we apply the canonical transformation to the Hamiltonian in order to obtain the small-polaron type of the external electron self-energy, but we also calculate the first correction to this term which could have an important role in the case of *electron* lattice.

The layout of the paper is as follows. In Sec. II we define the Hamiltonian for our system and put it in the form appropriate for further transformation by dividing it into dynamical and static parts. The appropriate tight-binding approach is elaborated in Sec. III, resulting in the closed expression for the total energy of the system which explicitly includes the polaron dispersion. The external electron wave function is given in Sec. IV as a sum over the complete set of exactly orthonormalized Wannier functions. In Sec. V we calculate and discuss our results and compare them with those derived in I. The conclusion is given in Sec. VI.

II. MODEL HAMILTONIAN

We analyze the interaction of the external electron e, placed at a lateral position $\boldsymbol{\rho}$ and at a distance z above the dielectric surface, with electrons of a Wigner lattice. The Hamiltonian of this system:

$$H = H_L + H_e + H_{eL} \tag{1}$$

is discussed in detail in I. For the sake of clarity we shall briefly explain the main terms, using the same notation as in I.

The term H_L is the lattice Hamiltonian. We assume that N electrons form a quasi-2D hexagonal Wigner lattice, deposited on a dielectric layer (e.g., liquid He) of thickness d and placed on a semiinfinite metallic substrate. Following the arguments given in I we factorize the lattice wave function into the lateral and perpendicular part. After averaging over the perpendicular component we find

$$\overline{H_L} = H_{\mathrm{osc}} + \langle E^{\mathrm{im}} \rangle + \frac{1}{2} \langle W^{ee} \rangle. \tag{2}$$

The first term

$$H_{\mathrm{osc}} = \sum_{\boldsymbol{\kappa}} \sum_p \hbar \omega_{\boldsymbol{\kappa}p} \left(a_{\boldsymbol{\kappa}p}^{\dagger} a_{\boldsymbol{\kappa}p} + \frac{1}{2} \right) \tag{3}$$

describes the energy of the two phonon modes $p = (+,-)$ of a Wigner lattice with frequencies $\omega_{\boldsymbol{\kappa}p}$. $\boldsymbol{\kappa}$ is the phonon wave vector in the I Brillouin zone (I BZ) and $a_{\boldsymbol{\kappa}p}(a_{\boldsymbol{\kappa}p}^{\dagger})$ are boson operators which annihilate (create) phonons. The term $\langle E^{\mathrm{im}} \rangle$ gives the z-averaged contribution of an image energy and the

term $\langle W^{ee} \rangle$ describes the z-averaged electrostatic repulsion of lattice electrons in their regular sites.

The Hamiltonian H_e of an external electron can also be divided into three main parts: kinetic energy K, image potential V^{im} and interaction U with lattice electrons in their regular sites. After averaging U over the perpendicular lattice electrons coordinates we find

$$\overline{H_e} = K + V^{\mathrm{im}}(z) + \bar{U}(\boldsymbol{\rho}, z). \tag{4}$$

As in the case of lattice electrons, we shall assume the external electron wave function to be a product of a perpendicular $u_e(z)$ and a parallel $\psi_e(\boldsymbol{\rho})$ components. For the perpendicular ground state, $u_e(z)$ has a standard form:

$$u_e(z) = 2\alpha_e^{3/2} z \exp(-\alpha_e z), \tag{5}$$

where α_e is the variational parameter which determines a perpendicular delocalization of the external electron.

Dividing kinetic energy operator K into its parallel $K_{\parallel}$ and perpendicular $K_{\perp}$ components and averaging Hamiltonian (4) with $u_e(z)$ we obtain

$$H_e(\boldsymbol{\rho}) = K_{\parallel}(\boldsymbol{\rho}) + \langle \epsilon^{\mathrm{im}} \rangle + \langle W_0 \rangle + \Delta U(\boldsymbol{\rho}). \tag{6}$$

The z-averaged value of $(K_{\perp} + V^{\mathrm{im}})$ gives the image energy $\langle \epsilon^{\mathrm{im}} \rangle$ of the external electron, while the z-averaged periodic potential U can be expanded into a Fourier series, where the summation is performed over all reciprocal lattice vectors $\mathbf{G}$. In this expansion $\langle W_0 \rangle$ represents the $\mathbf{G}=0$ term of electron-electron interaction and the $\boldsymbol{\rho}$-dependent term of U is

$$\Delta U(\boldsymbol{\rho}) = \sum_{\mathbf{G} \neq 0} \langle W(\mathbf{G}) \rangle e^{i\mathbf{G}\boldsymbol{\rho}}. \tag{7}$$

It contains all $\mathbf{G} \neq 0$ Fourier components $\langle W(\mathbf{G}) \rangle$ of the z-averaged interaction of the external electron with lattice electrons in their regular sites.

The term H_{eL} in Eq. (1) describes the dynamical part of the external electron interaction with lattice electrons. After averaging over z it takes the standard form of the electron-phonon interaction:[10]

$$H_{eL}(\boldsymbol{\rho}) = \sum_{\mathbf{k}} \sum_p e^{i\mathbf{k}\boldsymbol{\rho}} M_{\mathbf{k}p} (a_{\boldsymbol{\kappa}p} + a_{-\boldsymbol{\kappa}p}^{\dagger}), \tag{8}$$

where the z-averaged matrix elements are:

$$M_{\mathbf{k}p} = \frac{1}{\sqrt{N}} \langle W(\mathbf{k}) \rangle \left(\frac{\hbar}{2m\omega_{\boldsymbol{\kappa}p}} \right)^{1/2} k \cos \Phi_p(\mathbf{k}, \boldsymbol{\kappa}). \tag{9}$$

The angle $\Phi_p(\mathbf{k}, \boldsymbol{\kappa})$ is defined as the angle between the Fourier wave vector $\mathbf{k} = \boldsymbol{\kappa} + \mathbf{G}$ and the direction of the $(\boldsymbol{\kappa}, p)$ mode polarization.

Notice that the z-averaging in the Hamiltonians $H_e(\boldsymbol{\rho})$ (6) and $H_{eL}(\boldsymbol{\rho})$ (8) is performed with perpendicular wave functions of both lattice electrons and the external electron (5). Therefore the z-averaged terms in those Hamiltonians depend upon the variational parameter α_e, which we shall determine later, and upon the corresponding lattice parameter (α), which was calculated and discussed in I.

The total Hamiltonian (1) of our system is now transformed into

$$H(\boldsymbol{\rho}) = \overline{H_L} + H_e(\boldsymbol{\rho}) + H_{eL}(\boldsymbol{\rho}) = H_{\text{din}} + \langle E^{\text{stat}} \rangle, \qquad (10)$$

where

$$H_{\text{din}} = H_{\text{osc}} + K_{\parallel}(\boldsymbol{\rho}) + \Delta U(\boldsymbol{\rho}) + H_{eL}(\boldsymbol{\rho}) \qquad (11)$$

represents the dynamical part of the system, while

$$\langle E^{\text{stat}} \rangle = \langle E^{\text{im}} \rangle + \frac{1}{2} \langle W^{ee} \rangle + \langle e^{\text{im}} \rangle + \langle W_0 \rangle \qquad (12)$$

denotes the static part, which does not contain either the lattice phonon operators or the parallel coordinate of the external electron.

III. TIGHT-BINDING APPROACH

Let us expand the external electron wave function $\Psi_e(\boldsymbol{\rho})$ over a complete set of orthonormalized functions $\psi_j(\boldsymbol{\rho})$. As a complete set we can take, e.g., the Bloch functions $\psi_{\boldsymbol{\kappa}_e}(\boldsymbol{\rho})$, where $\boldsymbol{\kappa}_e$ denotes the Bloch wave vector in the I BZ, or the Wannier functions $\psi_W(\boldsymbol{\rho} - \boldsymbol{\rho}_j^0)$, defined for each regular lattice point $\boldsymbol{\rho}_j^0$:

$$\Psi_e(\boldsymbol{\rho}) = \sum_{\boldsymbol{\kappa}_e} \psi_{\boldsymbol{\kappa}_e}(\boldsymbol{\rho}) c_{\boldsymbol{\kappa}_e} = \sum_j \psi_W(\boldsymbol{\rho} - \boldsymbol{\rho}_j^0) c_j. \qquad (13)$$

Here $c_{\boldsymbol{\kappa}_e}(c_j)$ are fermion annihilation operators in the Bloch (Wannier) representation, respectively.

In I we have treated H_{eL} as a perturbation, so $\Psi_e(\boldsymbol{\rho})$ was the solution for the static periodic potential. In Ref. 8 we have shown that in the case of strictly 2D Wigner lattice better results are obtained when the electron-phonon interaction is (partly) included in the unperturbed Hamiltonian. This latter approach is generally preferred when the electron-phonon interaction plays a particularly important role. Assuming such a situation here, we shall diagonalize the main part of H_{eL} following the ''small-polaron theory.''[10] In some steps we shall generalize this theory so that we could take into account the specific properties of an *electronic* lattice, also quoting the standard approximations in the ''small-polaron'' approaches for *atomic* lattices.

We start by representing the electron wave function (13) by Wannier functions. This affects the last three terms in the dynamical part of the Hamiltonian (11) which contain the external electron coordinate. Therefore we can write H_{din} in the second-quantized form as

$$H_{\text{din}} = H_{\text{osc}} + \sum_j \sum_{\boldsymbol{\delta}} c_{j+\boldsymbol{\delta}}^{\dagger} c_j [K_{\parallel}(\boldsymbol{\delta}) + \Delta U(\boldsymbol{\delta}) + H_{eL}^j(\boldsymbol{\delta})]. \qquad (14)$$

By $\boldsymbol{\delta} = (\boldsymbol{\rho}_i^0 - \boldsymbol{\rho}_j^0)$ we denote the difference between any two regular lattice points. The energy terms in Eq. (14) can be written in both the direct and Fourier space as

$$K_{\parallel}(\boldsymbol{\delta}) = \int d\boldsymbol{\rho} \Phi_W^*(\boldsymbol{\rho} - \boldsymbol{\delta}) K_{\parallel}(\boldsymbol{\rho}) \Phi_W(\boldsymbol{\rho})$$

$$= n \frac{1}{N} \sum_{\mathbf{k}} \frac{\hbar^2 k^2}{2m} e^{ik\delta} |\Phi_W(\mathbf{k})|^2, \qquad (15)$$

$$\triangle U(\boldsymbol{\delta}) = \int d\boldsymbol{\rho} \Phi_W^*(\boldsymbol{\rho} - \boldsymbol{\delta}) \triangle U(\boldsymbol{\rho}) \Phi_W(\boldsymbol{\rho})$$

$$= n \sum_{\mathbf{G} \neq 0} \langle W(\mathbf{G}) \rangle g_{\mathbf{G}}(\boldsymbol{\delta}), \qquad (16)$$

$$H_{eL}^j(\boldsymbol{\delta}) = \int d\boldsymbol{\rho} \Phi_W^*(\boldsymbol{\rho} - \boldsymbol{\rho}_j^0 - \boldsymbol{\delta}) H_{eL}(\boldsymbol{\rho}) \Phi_W(\boldsymbol{\rho} - \boldsymbol{\rho}_j^0)$$

$$= \sum_{\boldsymbol{\kappa}} \sum_p e^{i\boldsymbol{\kappa}\boldsymbol{\rho}_j^0} M_{\boldsymbol{\kappa}p}(\boldsymbol{\delta}) (a_{\boldsymbol{\kappa}p} + a_{-\boldsymbol{\kappa}p}^{\dagger}), \qquad (17)$$

where we have introduced the ''overlap'' function:

$$g_{\mathbf{k}}(\boldsymbol{\delta}) = \int d\boldsymbol{\rho} \Phi_W^*(\boldsymbol{\rho} - \boldsymbol{\delta}) \Phi_W(\boldsymbol{\rho}) e^{ik\rho}$$

$$= \frac{1}{n} \frac{1}{N} \sum_{\mathbf{k}'} \Phi_W^*(\mathbf{k}') \Phi_W(\mathbf{k}' - \mathbf{k}) e^{ik'\delta}. \qquad (18)$$

Notice that in the extreme tight-binding limit $g_{\mathbf{k}}(\boldsymbol{\delta})$ differs from zero only for $\boldsymbol{\delta} = 0$, which gives the diagonal part of the Hamiltonian (14).

The generalized matrix elements in Eq. (17):

$$M_{\boldsymbol{\kappa}p}(\boldsymbol{\delta}) = \sum_{\mathbf{G}} g_{\boldsymbol{\kappa}+\mathbf{G}}(\boldsymbol{\delta}) M_{\boldsymbol{\kappa}+\mathbf{G}p} \qquad (19)$$

satisfy symmetry relation: $M_{-\boldsymbol{\kappa}p}(-\boldsymbol{\delta}) = \exp(i\boldsymbol{\kappa}\boldsymbol{\delta}) M_{\boldsymbol{\kappa}p}^*(\boldsymbol{\delta})$, which for real Wannier functions transforms into standard relation: $M_{-\boldsymbol{\kappa}p}(\boldsymbol{\delta}) = M_{\boldsymbol{\kappa}p}^*(\boldsymbol{\delta})$.

The term $H_{eL}^j(\boldsymbol{\delta})$ depends explicitly on the lattice coordinate $\boldsymbol{\rho}_j^0$ and the phonon operators $a_{\boldsymbol{\kappa}p}, a_{\boldsymbol{\kappa}p}^{\dagger}$, so that the Hamiltonian (14) cannot be exactly diagonalized. In order to diagonalize the main part of electron-phonon interaction we shall apply the canonical transformation:[10]

$$H_{\text{din}}^T = e^{-S} H_{\text{din}} e^S,$$

$$S = \sum_j c_j^{\dagger} c_j \sum_{\boldsymbol{\kappa}} \sum_p S_{\boldsymbol{\kappa}p}^j (a_{\boldsymbol{\kappa}p} - a_{-\boldsymbol{\kappa}p}^{\dagger}),$$

$$S_{\boldsymbol{\kappa}p}^j = e^{i\boldsymbol{\kappa}\boldsymbol{\rho}_j^0} \frac{M_{\boldsymbol{\kappa}p}(0)}{\hbar \omega_{\boldsymbol{\kappa}p}}. \qquad (20)$$

Operator S contains only $\boldsymbol{\delta} = 0$ term, but all $\mathbf{G}$ terms are included in $M_{\boldsymbol{\kappa}p}(0)$. For atomic lattices only $\mathbf{G} = 0$ term is usually taken into account.

The transformation (20) simply shifts the phonon operators: $a_{\boldsymbol{\kappa}p}^T = a_{\boldsymbol{\kappa}p} - \Sigma_j c_j^{\dagger} c_j S_{\boldsymbol{\kappa}p}^j$ while the fermion operators are changed as: $c_j^T = X_j c_j = c_j X_j$, where X_j is the unitary operator:

$$X_j = \exp\left[\sum_{\boldsymbol{\kappa}} \sum_p S_{\boldsymbol{\kappa}p}^j (a_{\boldsymbol{\kappa}p} - a_{-\boldsymbol{\kappa}p}^{\dagger}) \right].$$

The transformed Hamiltonian (20) takes the form

$$H_{\text{din}}^T = H_{\text{osc}} + \sum_j c_j^{\dagger} c_j \epsilon_0^{eL} + \sum_j \sum_{\boldsymbol{\delta}} c_{j+\boldsymbol{\delta}}^{\dagger} c_j$$

$$\times [K_{\parallel}(\boldsymbol{\delta}) + \Delta U(\boldsymbol{\delta})] X_{j+\boldsymbol{\delta}}^{\dagger} X_j + H_{eL}'^T. \qquad (21)$$

In Eq. (21) we have extracted the $\delta = 0$ term from electron-phonon interaction H_{eL}^T, so that this term together with a part of lattice Hamiltonian H_{osc}^T gives the standard polaron self-energy[10]

$$\epsilon_0^{eL} = -\sum_{\kappa} \sum_p \frac{1}{\hbar \omega_{\kappa p}} |M_{\kappa p}(0)|^2. \qquad (22)$$

The remaining term $H_{eL}^{\prime T}$ in Eq. (21) describes the part of electron-phonon interaction which involves electron coordinates at two different lattice cells ($\delta \neq 0$) and therefore in the tight-binding approximation is supposed to give much smaller contribution to the electron energy than the polaron self-energy (22). In standard calculations this term is usually neglected, but in the case of electron lattice we expect that its contribution to the electron energy could be even more important than the contribution from the nondiagonal ($\delta \neq 0$) terms of electron kinetic and potential energy. After some manipulation we find

$$H_{eL}^{\prime T} = \sum_j \sum_{\delta \neq 0} c_{j+\delta}^\dagger c_j X_{j+\delta}^\dagger X_j \sum_{\kappa} \sum_p$$
$$\times [e^{i\kappa \rho_j^0} M_{\kappa p}(\delta)(a_{\kappa p} + a_{-\kappa p}^\dagger) - 2\epsilon_{\kappa p}^M(\delta)],$$

$$\epsilon_{\kappa p}^M(\delta) = \frac{M_{\kappa p}(\delta) M_{\kappa p}^*(0)}{\hbar \omega_{\kappa p}}. \qquad (23)$$

Although we expect that the external eletron will be well localized between lattice electrons,[5] we have made no such assumption yet, i.e., Hamiltonians (11) and (21) are exactly equivalent. At this point we shall assume that the canonical transformation (20) enables us to take the phonon ground state $|0_{ph}\rangle$ as a good approximation for the ground state of the system. It is clearly the exact phonon ground state of the Hamiltonian (21) if only $\delta = 0$ terms are taken into account. Note that if we transform the state vectors instead of the Hamiltonian, we find that the canonical transformation (20) pushes the unperturbed phonons into their coherent states: $|0_{coh}\rangle = e^S |0_{ph}\rangle$, in which the main ($\delta = 0$) part of electron-phonon interaction gives an energy shift (22).

Now we wish to determine the corrections to the ground state energy due to the contribution of various $\delta \neq 0$ terms. First we calculate

$$\langle 0_{ph} | X_{j+\delta}^\dagger X_j | 0_{ph} \rangle = \exp[-S_0(\delta)]$$

which gives[10]

$$S_0(\delta) = \sum_{\kappa} \sum_p [1 - \cos(\kappa \delta)] \frac{|M_{\kappa p}(0)|^2}{(\hbar \omega_{\kappa p})^2}. \qquad (24)$$

After lengthy but straightforward calculations we find the next needed average

$$\langle 0_{ph} | X_{j+\delta}^\dagger X_j \sum_{\kappa} \sum_p [e^{i\kappa \rho_j^0} M_{\kappa p}(\delta)(a_{\kappa p} + a_{-\kappa p}^\dagger)] | 0_{ph} \rangle$$

$$= e^{-S_0(\delta)} \sum_{\kappa} \sum_p (1 - e^{-i\kappa \delta}) \epsilon_{\kappa p}^M(\delta).$$

It enables us to write the contribution from the ''overlap'' $\delta \neq 0$ terms of the electron-phonon interaction (23) in the transparent form:

$$\langle 0_{ph} | H_{eL}^{\prime T} | 0_{ph} \rangle = \sum_j \sum_{\delta \neq 0} c_{j+\delta}^\dagger c_j e^{-S_0(\delta)} \epsilon^{eL}(\delta),$$

$$\epsilon^{eL}(\delta) = \sum_{\kappa} \sum_p (1 + e^{-i\kappa \delta}) \epsilon_{\kappa p}^M(\delta). \qquad (25)$$

Notice that $\epsilon^{eL}(0) = 2\epsilon_0^{eL}$.

Finally we can write the zero-phonon average of the Hamiltonian (21):

$$\langle 0_{ph} | H_{din}^T | 0_{ph} \rangle = \langle E^{osc} \rangle + \epsilon_0^{din} \sum_j c_j^\dagger c_j + \sum_j \sum_{\delta \neq 0} e^{-S_0(\delta)}$$
$$\times [K_\parallel(\delta) + \Delta U(\delta) + \epsilon^{eL}(\delta)] c_{j+\delta}^\dagger c_j, \qquad (26)$$

where $\langle E^{osc} \rangle$ is the standard zero-phonon contribution of the unperturbed lattice Hamiltonian (3), calculated in Ref. 11, and

$$\epsilon_0^{din} = \epsilon_0^{eL} + K_\parallel(0) + \Delta U(0). \qquad (27)$$

The terms in the Hamiltonian (26) do not depend explicitly upon the lattice coordinates and the summation over j includes only the operators $c_{j+\delta}^\dagger c_j$. Therefore we can diagonalize the Hamiltonian (26) if we introduce the Bloch instead of Wannier operators, as defined in Eq. (13). It gives

$$\langle 0_{ph} | H_{din}^T | 0_{ph} \rangle = \langle E^{osc} \rangle + \sum_{\kappa_e} [\epsilon_0^{din} + \epsilon^{din}(\kappa_e)] c_{\kappa_e}^\dagger c_{\kappa_e}. \qquad (28)$$

The second term in Eq. (28) represents the dynamical part of the external electron energy. In the Bloch state $|\kappa_e\rangle$ it is given as a sum of the ''nonoverlap'' ($\delta = 0$) contribution ϵ_0^{din} (27) which does not depend upon κ_e, and the ''overlap'' ($\delta \neq 0$) contribution which depends upon κ_e as

$$\epsilon^{din}(\kappa_e) = \sum_{\delta \neq 0} e^{-S_0(\delta)} [K_\parallel(\delta) + \Delta U(\delta) + \epsilon^{eL}(\delta)] e^{-i\kappa_e \delta}. \qquad (29)$$

Obviously, $\epsilon^{din}(\kappa_e)$ is real because all energy terms in Eq. (29) satisfy $\epsilon(-\delta) = \epsilon^*(\delta)$.

Assuming that the system (Wigner lattice + external electron) is in the state $|0_{ph}\rangle |\kappa_e\rangle$, the total energy of the system follows from Eqs. (10) and (28): $E^{tot} = E^{stat} + \langle E^{osc} \rangle + \epsilon_0^{din} + \epsilon^{din}(\kappa_e)$, or more conveniently we can divide it into the E^L (lattice) and E^{eL} (external electron + interaction) contribution:

$$E^{tot} = E^L + E^{eL}(\kappa_e), \qquad (30)$$

$$E^L = \langle E^{im} \rangle + \frac{1}{2} \langle W^{ee} \rangle + \langle E^{osc} \rangle, \qquad (31)$$

$$E^{eL}(\kappa_e) = \langle e^{im} \rangle + \langle W_0 \rangle + \epsilon_0^{din} + \epsilon^{din}(\kappa_e). \qquad (32)$$

IV. POLARON WAVE FUNCTION

In order to calculate the energy of the external electron in the $|0_{ph}\rangle|\kappa_e\rangle$ state of the system we first have to determine the wave function of the Bloch state $|\kappa_e\rangle$. Following I, we put

$$\psi_{\kappa_e}(\boldsymbol{\rho}) = \frac{1}{\sqrt{N}} \sum_j \Phi_{\kappa_e}(\boldsymbol{\rho} - \boldsymbol{\rho}_j^0) e^{i\kappa_e \rho_j^0}. \tag{33}$$

Although we assume that $\Phi_{\kappa_e}(\boldsymbol{\rho})$ depends explicitly on κ_e, the wave function (33) satisfies the Bloch theorem for any $\Phi_{\kappa_e}(\boldsymbol{\rho})$. We also need the corresponding Wannier function:

$$\psi_W(\boldsymbol{\rho}) = \frac{1}{N} \sum_{\kappa_e} \sum_j \Phi_{\kappa_e}(\boldsymbol{\rho} - \boldsymbol{\rho}_j^0) e^{i\kappa_e \rho_j^0}. \tag{34}$$

Notice that the Fourier components of $\psi_W(\boldsymbol{\rho})$:

$$\psi_W(\mathbf{k}) \equiv \psi_W(\kappa + \mathbf{G}) = \Phi_\kappa(\kappa + \mathbf{G}) \tag{35}$$

are not the Fourier components of a single function $\Phi_{\kappa_e}(\boldsymbol{\rho})$ because in Eq. (35) we have the same wave vector $\kappa_e = \kappa$ in the subscript and in the argument of the function Φ_κ. Particularly, if we assume that $\Phi_{\kappa_e}(\boldsymbol{\rho})$ does not depend upon κ_e, it would represent the true Wannier function $\psi_W(\boldsymbol{\rho}) = \Phi_{\kappa_e}(\boldsymbol{\rho})$, as discussed in I.

The functions $\Psi_W(\boldsymbol{\rho})$ should be normalized, which gives in the direct and in the reciprocal space, for any κ:

$$\sum_\delta e^{-i\kappa\delta} \int d\boldsymbol{\rho} \Phi_\kappa^*(\boldsymbol{\rho} - \delta) \Phi_\kappa(\boldsymbol{\rho}) = 1, \tag{36}$$

$$n \sum_{\mathbf{G}} |\Phi_\kappa(\kappa + \mathbf{G})|^2 = 1. \tag{37}$$

To this point we have made no assumption about the external electron wave function. It is uniquely specified in Bloch (33) or in Wannier (34) form by the tight-binding function $\Phi_{\kappa_e}(\boldsymbol{\rho})$. Following I, we expect that the external electron, being repelled from the regular lattice sites, is localized somewhere around the two points in each lattice cell where it has a minimum potential energy (Fig. 1), so we can write

$$\Phi_{\kappa_e}(\boldsymbol{\rho}) = C_{\kappa_e} \sum_l \phi_{\kappa_e}(\boldsymbol{\rho} - \mathbf{s}_l). \tag{38}$$

In order to preserve the C_6 symmetry of the hexagonal Wigner lattice when the overlap of the tight-binding functions is taken into account, instead over two lattice points, we actually have to sum over six lattice points[8] $\{\mathbf{s}_l, l = 1, 2 \dots 6\}$ which form the hexagon around each lattice electron (Fig. 1). The potential energy of the external electron is nearly harmonic around these points so we put[5]

$$\phi_{\kappa_e}(\boldsymbol{\rho}) = \exp(-\rho^2/2\sigma_{\kappa_e}^2), \tag{}$$

where σ_{κ_e} is the lateral delocalization parameter which we shall determine later by the variational calculation.

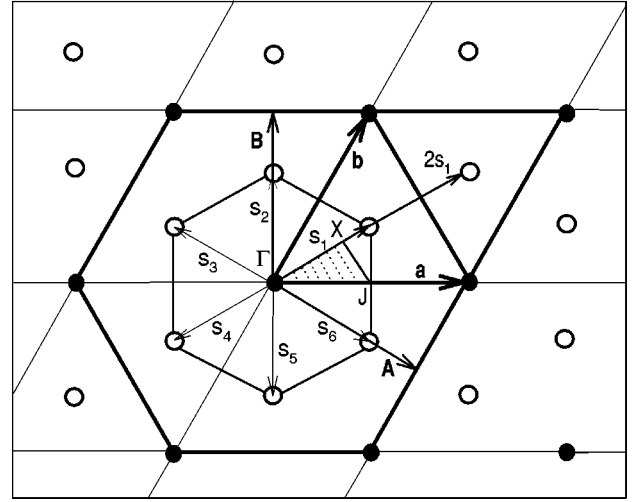Now we can find the Fourier transform of $\Phi_{\kappa_e}(\boldsymbol{\rho})$:

FIG. 1. 2D hexagonal lattice with primitive vectors $\mathbf{a}, \mathbf{b}$. Full circles represent regular positions of lattice electrons and empty circles the most probable positions of an external electron. Also shown are reciprocal lattice vectors $\mathbf{A}, \mathbf{B}$ and the irreducible part of the I BZ, determined by the special points Γ, X and J.

$$\Phi_{\kappa_e}(\mathbf{k}) = n 2 \pi \sigma_{\kappa_e}^2 C_{\kappa_e} \sum_l e^{-i k s_l} \exp(-\sigma_{\kappa_e}^2 k^2/2), \tag{}$$

which for $\kappa_e = \kappa$ also gives the Fourier transform (35) of the Wannier function.

The coefficient C_κ in Eq. (38) follows from the normalization condition (36) or (37):

$$C_\kappa = \frac{1}{\sqrt{\pi}\sigma_\kappa} C_\kappa', \tag{}$$

$$C_\kappa'^{-2} = \sum_\delta e^{-i\kappa\delta} \sum_l \sum_{l'} \exp[-(\delta + \mathbf{s}_{l'} - \mathbf{s}_l)^2/4\sigma_\kappa^2]$$
$$= 4\pi n \sigma_\kappa^2 \sum_{\mathbf{G}} \exp[-\sigma_\kappa^2(\kappa + \mathbf{G})^2] \left| \sum_l e^{-i(\kappa + \mathbf{G})s_l} \right|^2. \tag{39}$$

The dimensionless coefficient C_κ' is given in both δ and $\mathbf{G}$ expansions. At some specific κ values it happens that the leading terms in one expansion are canceled so one should use another expansion to precisely determine C_κ'.

From now on we shall assume that delocalization parameter $\sigma_{\kappa_e} = \sigma_e$ does not depend upon κ_e, so $\Phi_{\kappa_e}(\boldsymbol{\rho})$ will depend upon κ_e through the coefficient (39). In I we have used the Bloch function with the $\sigma(\kappa_e)$ dependence determined from the behavior of an external electron in a static periodic potential. This dependence was rather smooth, which also justifies our assumption. The same assumption was also successfully applied in Ref. (8).

The Wannier function $\Psi^W(\boldsymbol{\rho})$ is shown in Fig. 2. For $r_0 = 100$ Å we put the (optimum) value $\sigma_e = 16$ Å (Fig. 3). With the same parameters and for $\kappa_e = 0$ we also show the tight-binding function $\Phi_{\kappa_e=0}(\boldsymbol{\rho})$ and the Bloch function $\Psi_{\kappa_e=0}(\boldsymbol{\rho})$, which takes a simple form:
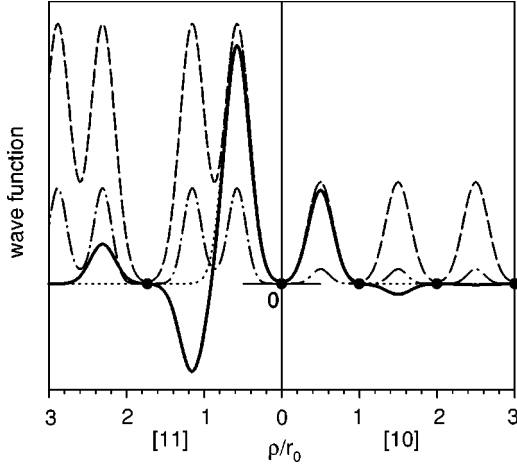
FIG. 2. The Wannier wave function Ψ^W (full line) compared with the tight-binding function $\Phi_{\kappa_e=0}$ (dotted line) and the Bloch function (arbitrary scale) $\Psi_{\kappa_e=0}$ (dashed line). Also shown is the electron density $|\Psi_{\kappa_e=0}|^2$ (dashed-dotted line). The functions are shown along the two different directions [10] and [11] of a Wigner lattice and full circles represent regular positions of lattice electrons in these directions.

$$\Psi_{\kappa_e=0}(\boldsymbol{\rho}) = \frac{1}{\sqrt{N}} \sum_j \Psi^W(\boldsymbol{\rho} - \boldsymbol{\rho}_j^0) = \frac{1}{\sqrt{N}} \sum_j \Phi_{\kappa_e=0}(\boldsymbol{\rho} - \boldsymbol{\rho}_j^0).$$

As expected, wave functions have zeros at the regular positions of lattice electrons. Notice that $\Psi^W(\boldsymbol{\rho})$ and $\Phi_{\kappa_e=0}(\boldsymbol{\rho})$ are almost the same at the first maximum, but further from that point $\Phi_{\kappa_e=0}(\boldsymbol{\rho})$ decreases exponentially while $\Psi^W(\boldsymbol{\rho})$ oscillates in order to satisfy the orthogonality requirement. These oscillations decay showing local maxima (minima) at points that are equally separated from the neighboring lattice electrons. Precisely at those points $\Psi_{\kappa_e=0}(\boldsymbol{\rho})$ has also maxima, but for $\kappa_e=0$ they are all of the same intensity. The corresponding density of the external electron $|\Psi_{\kappa_e=0}(\boldsymbol{\rho})|^2$ is well localized between the lattice electrons.
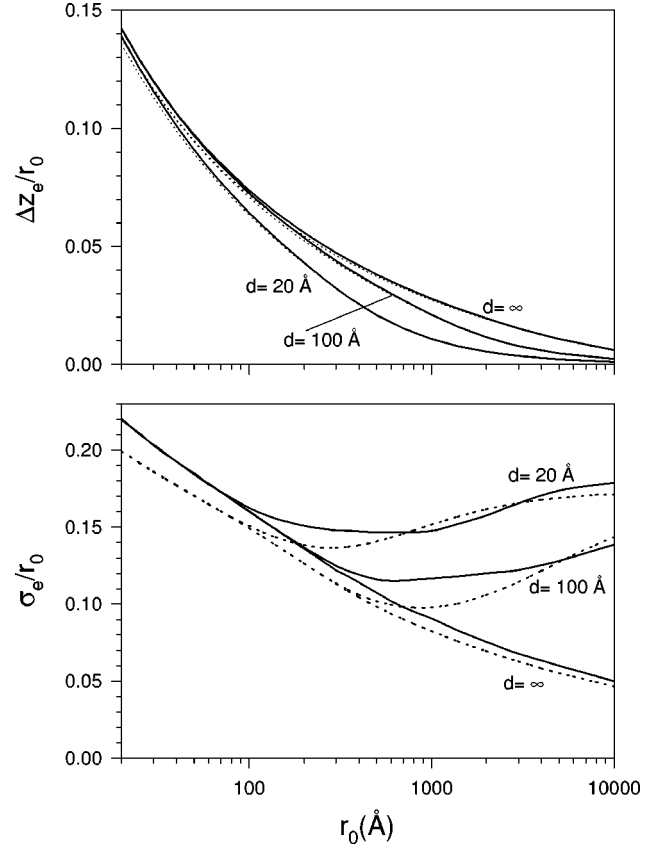

FIG. 3. Relative spread $\Delta z_e/r_0$ and σ_e/r_0 of an external electron wave function as a function of r_0, for three different thicknesses d of a dielectric layer (liquid He). Dotted lines represent corresponding values derived in I.

We stress that this intuitively expected behavior was derived with only one parameter (σ_e), determined uniquely by the variational calculation.

V. RESULTS AND DISCUSSION

Knowing the external electron wave function we can calculate the electron energy as a function of a Bloch wave vector κ_e. Let us first calculate $g_{\mathbf{k}}(\boldsymbol{\delta})$ which enters either directly or through $M_{\mathbf{k}p}(\boldsymbol{\delta})$ in various energy terms:

$$g_{\boldsymbol{\kappa}+\mathbf{G}}(\boldsymbol{\delta}) = \frac{1}{N} \sum_{\boldsymbol{\kappa}'} e^{i\boldsymbol{\kappa}'\boldsymbol{\delta}} C'^*_{\boldsymbol{\kappa}'} C'_{\boldsymbol{\kappa}'-\boldsymbol{\kappa}} \exp[-\sigma_e^2(\boldsymbol{\kappa}+\mathbf{G})^2/4] \sum_{\boldsymbol{\delta}'} \cos[\boldsymbol{\delta}'(-\boldsymbol{\kappa}'+\boldsymbol{\kappa}/2+\mathbf{G}/2)]$$

$$\times \sum_l \sum_{l'} \exp[-(\boldsymbol{\delta}'+\mathbf{s}_{l'}-\mathbf{s}_l)^2/4\sigma_e^2] e^{i(\mathbf{s}_{l'}+\mathbf{s}_l)(\boldsymbol{\kappa}+\mathbf{G})/2}$$

$$= \frac{1}{N} \sum_{\boldsymbol{\kappa}'} e^{i\boldsymbol{\kappa}'\boldsymbol{\delta}} 4\pi n \sigma_e^2 C'^*_{\boldsymbol{\kappa}'} C'_{\boldsymbol{\kappa}'-\boldsymbol{\kappa}} \sum_{\mathbf{G}'} \exp[-\sigma_e^2(\boldsymbol{\kappa}'-\mathbf{G}')^2/2 - (\boldsymbol{\kappa}'-\boldsymbol{\kappa}+\mathbf{G}'-\mathbf{G})^2/2]$$

$$\times \sum_l \sum_{l'} e^{i[(\boldsymbol{\kappa}'+\mathbf{G}')\mathbf{s}_{l'} - (\boldsymbol{\kappa}'-\boldsymbol{\kappa}+\mathbf{G}'-\mathbf{G})\mathbf{s}_l]}.$$

To calculate $g_{\kappa+G}(\delta)$ we have to sum over wave vectors κ' and over direct (δ') or reciprocal (G') lattice vectors. Whether we shall sum over δ' or G' depends upon σ_e and r_0: for $2\sigma_e/r_0 < (>)1$ the expansion over $\delta'(G')$ converges faster, respectively. The summation over κ' is transformed into integration in a standard way and it must be performed over the whole I BZ. To obtain various energy terms we have to sum again over G and over κ. Due to the symmetry, the summation over κ could be performed over the irreducibile part of the I BZ[12] only in the case $\kappa_e=0$, e.g., for ϵ_0^{din}.

A. Delocalization parameters

Now we are ready to calculate the perpendicular α_e and lateral σ_e delocalization parameters from the variational principle, by minimizing the total energy of the system (30) in its ground state $|0_{ph}\rangle|\kappa_e=0\rangle$. In fact we have to minimize only the part of E^{tot} which contains the contribution from the external electron, or, as denoted in I, the chemical potential of the external electron:

$$\mu_e \equiv E^{eL}(\kappa_e=0)$$
$$= \langle\epsilon^{im}\rangle + \langle W_0\rangle + K_\parallel(0) + \Delta U(0) + \epsilon_0^{eL} + \epsilon^{din}(\kappa_e=0). \tag{40}$$

The first two terms depend only upon α_e, the third term depends only upon σ_e while other terms depend upon both parameters, which means that the minimization procedure should be performed simultaneously.

Calculated perpendicular $\Delta z_e = \sqrt{3}/2\,\alpha_e$ and lateral σ_e spread of the external electron wave function are shown on Fig. 3, together with the corresponding values derived in I. The α_e values are almost the same in both cases as a consequence of the same shape of the image potential which mainly determines the perpendicular delocalization. The new σ_e values are generally somewhat larger because they are derived from the electron energy (40) which contains the electron-phonon interaction, and it was not the case in I. However, for $r_0 > 20$ Å the external electron still remains well localized between the lattice electrons ($\sigma_e/r_0 < 0.22$, $\Delta z_e/r_0 < 0.14$), which was also demonstrated in Fig. 2. The electron localization is important because *a posteriori* it verifies the tight-binding approach.

B. Wigner phase transition

The optimum values of α_e and σ_e determine the properties of the external electron in the ground state of the system. From those properties we shall first try to determine the critical density parameter r_c for the $T=0$ Wigner phase transition, i.e., the transition from an electron solid into an electron gas due to increased electron density. There was a considerable interest for this problem in the last few years. Similarly as in the classical Kosterlitz-Thouless melting theory,[13] some theoretical approaches explain the $T=0$ Wigner transition as driven by the spontaneous generation and dissociation of dislocation pairs.[14] Other approaches calculate, e.g., the change in energy due to the point defects,[15] or use self-consistent Hartree-Fock[16] or density-functional[17] theory. The calculations are usually performed for the strictly 2D electrons and

the results are then compared with the first-principle calculations which determine separately the ground-state energies of the 2D electron lattice and the 2D electron gas as functions of electron density. The crossing point between those curves can be taken as the definition for the critical density parameter and the improved variational Monte Carlo calculations give $r_c = 37 \pm 5$.[9] Similar values are derived from different theories with different melting mechanisms, but some calculations also predict significantly lower values.[16] Evidently, the definite answer is yet not given and one could even expect that various melting mechanisms could act together to destroy the Wigner lattice.

Following the theory developed in I, we can calculate r_c by comparing the ground-state energy μ_e of the external electron added in between the lattice electrons, with the chemical potential μ_L of a perfect Wigner lattice. This comparison will show whether the external electron will become localized as one of the $(N+1)$ regular lattice electrons ($\mu_L < \mu_e$), or will prefer to stay delocalized as a polaron ($\mu_L > \mu_e$). In the last case the lattice potential can no longer trap the external electron, so in our approach $\mu_L = \mu_e$ indicates the beginning of the lattice melting and we take it as a definition for the critical density parameter.

As in I, we shall first extract the $\langle W_0^d\rangle$ term from both μ_e and μ_L. Here $\langle W_0^d\rangle$ is a part of an average electron-electron interaction $\langle W_0\rangle$, which depends only upon the properties of a dielectric substrate. This extraction can be done analytically, so the renormalized quantities $\mu_e' = \mu_e - \langle W_0^d\rangle$ and $\mu_L' = \mu_L - \langle W_0^d\rangle$ can be compared much easier, as shown in Fig. 4.

In the *high-density* region, Fig. 4(a), the crossing of the μ_e' and μ_L' curves determines the critical lattice parameter r_0^c for the $T=0$ Wigner phase transition. This happens at $r_0^c \approx 36$ Å for $d=20$ Å, $r_0^c \approx 38$ Å for $d=100$ Å, and $r_0^c \approx 43$ Å for $d=\infty$. [Notice that for 2D hexagonal lattice the density parameter r_s is practically the same as $r_0(Å):r_s = 0.992 r_0(Å)$, i.e., $r_c \approx r_0^c(Å)$.] Interestingly enough, all these calculated critical parameters are close to the value $r_c = 37$ obtained for the strictly 2D Wigner lattice.[9] It seems that the image potential caused by the substrate and the perpendicular spreading of the electron wave functions have no essential influence on the $T=0$ Wigner phase transition in the high-density region. As compared with our results derived in I, we find significant difference between the μ_e' curves for $d=20$ Å and almost no difference for $d=\infty$. Here the consistent treatment of the electron-phonon interaction gives higher polaron energies in the presence of a strong image potential ($d=20$ Å) thus giving higher μ_e' values than in I.

In the *low density* region, Fig. 4(b), our results are closely related to those derived in I. The curves μ_e' and μ_L' have the same asymptotic behavior and the crossing point is not sharply defined. A detailed inspection gives the crossing only for the $d=20$ Å curves at $r_0 \approx 1200$ Å. For $d=100$ Å the curves become practically the same for $r_0 > 2000$ Å (within the numerical error), and for $d=\infty$ there is definitely no crossing. We can conclude that at very low densities we shall have a Wigner lattice for $d=\infty$ and a 2D electron gas for $d=20$ Å. This is expected because at low electron densities and for thin dielectric films the image potential of a dipole
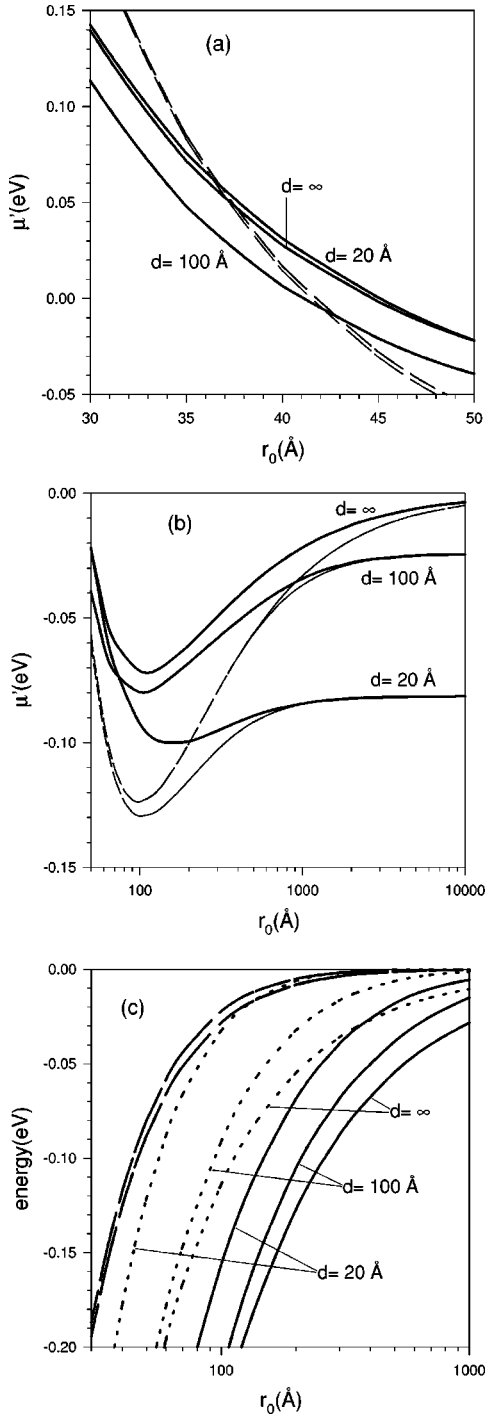
FIG. 5. Energy of the external electron $\Delta \epsilon_e$ as a function of the electron wave vector $\boldsymbol{\kappa}_e$ taken along the ΓX and ΓJ direction of the I BZ in units of a reciprocal lattice parameter $g_0 = 4\pi/\sqrt{3} r_0$. The curves are shown for three lattice parameters and for three He layers. The $d = 20$ Å curve for $r_0 = 3000$ Å is 10^4 times enlarged. Full lines: $\Delta \epsilon_e$ with electron-phonon term; dashed lines: $\Delta \epsilon_e$ without electron-phonon term; dotted lines: free-electron curves $\epsilon_0(\boldsymbol{\kappa}_e) = \hbar^2 \kappa_e^2 / 2m$.

electric layer leads to a weaker electron-electron interaction[11] and therefore to a *greater* (less negative) tight-binding contribution. However it also leads, e.g., to a *lower* phonon contribution,[18] which (partly) explains the "mixing" of energy curves with different d-values on Figs. 4(a) and 4(b).

Notice that $|\epsilon^{\text{din}}(0)| \ll |\epsilon_0^{\text{din}}|$, valid at all given electron densities, ensures good convergence for the tight-binding expansion. This expansion is expected to converge when the electron-phonon interaction dominates the electron kinetic energy.[10] In our case it holds because we take into consideration only lower electron densities ($r_0 > 20$ Å). Moreover, this density region also covers the critical density for the $T = 0$ Wigner phase transition.

C. Polaron dispersion

Together with the ground-state energy, one usually wants to calculate the polaron dispersion $E^{eL}(\boldsymbol{\kappa}_e)$, which determines, e.g., the effective mass and the energy bandwidth of the external electron. This term is usually hard to calculate, and in I we have determined the dispersion of the external electron in a static periodic potential of a Wigner lattice, neglecting electron-phonon interaction. One of the main motivations for this article was the inclusion of this term.

Figure 5 shows the calculated external electron energy measured from the bottom of the energy band: $\Delta \epsilon_e(\boldsymbol{\kappa}_e)$

FIG. 4. (a), (b) Renormalized chemical potential of an external electron μ_e' (full lines) and of a Wigner lattice μ_L' (dashed lines) as a function of r_0. The scale for r_0 is linear in the high density region (a), and logarithmic in the low density region (b). The $\mu_L'(r_0)$ curves on (a) are almost the same for $d = 100$ Å and $d = \infty$ and are both above the corresponding $d = 20$ Å curve. (c) Tight-binding terms: ϵ_0^{din} (full lines), $\epsilon^{\text{din}}(0)$ (dashed lines), and ϵ_0^{eL} (dotted lines). The $\epsilon^{\text{din}}(0)$ curves for $d = 100$ Å and $d = \infty$ are indistinguishable and lie below the corresponding $d = 20$ Å curve.

(electron + image) layer dominates so it can prevent the formation of the electron lattice.[18]

To demonstrate the influence of the typical tight-binding contribution on the external electron energy we show on Fig. 4(c) separately the terms ϵ_0^{din}, $\epsilon^{\text{din}}(0)$, and ϵ_0^{eL}. Thinner di-
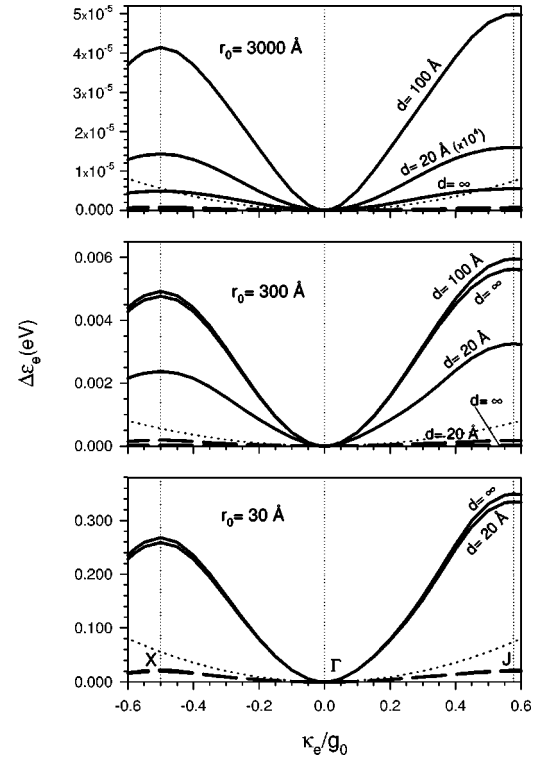
$\equiv E^{eL}(\boldsymbol{\kappa}_e) - E^{eL}(0) = \epsilon^{\mathrm{din}}(\boldsymbol{\kappa}_e) - \epsilon^{\mathrm{din}}(0)$. The influence of the electron-phonon interaction is clearly seen from the comparison of the dispersion curves with and without $\epsilon^{eL}(\boldsymbol{\delta})$ term. The $\Delta \epsilon_e(\boldsymbol{\kappa}_e)$ curves without this term show much less dispersion, resulting in an energy band much narrower than in the case of a free electron. As expected, the external electron, coherently ''dressed'' by phonons, has much larger effective mass than the free electron. However, with the nondiagonal electron-phonon contribution included, the total dispersion significantly increases. It means that the standard self-energy term (22) is not as good aproximation for the electron-phonon interaction in the Wigner (electron) lattice as it happens to be in the standard (atomic) lattice, so the correction to the standard self-energy cannot be neglected. Notice that the curves representing the dispersion of an ''undressed'' electron in a static periodic potential (Fig. 5 in I) fall in between the two types of curves shown here.

The comparison between the high-density ($r_0 = 30$ Å) and the lower density ($r_0 = 300$ Å) parts of Fig. 5 demonstrates the influence of the substrate. At high electron densities the dispersion is mainly determined by the direct electron-electron interaction so it is almost independent of d. At lower electron densities, as a consequence of the image potential, the dispersion depends upon the dielectric thickness. Notice that the curves without $\epsilon^{eL}(\boldsymbol{\delta})$ term show greater dispersion for $d = 20$ Å than for $d = \infty$. Lower d values mean greater influence of the image potential in comparison with a periodic lattice potential, so the external electron moves relatively more freely in the lateral direction.[5] But when $\epsilon^{eL}(\boldsymbol{\delta})$ term is included, lower d values also mean lower influence of this term so altogether we find a lower dispersion. As expected, the competition between the image potential and the polaron self-energy mainly determines the behavior of $\mu_e'(r_0)$ and $\Delta \epsilon_e(\boldsymbol{\kappa}_e)$ curves.

Further insight into the polaron dispersion one can obtain by comparing it with the dispersion of lattice phonons, which is shown in Fig. 6. Although calculated from quite different equations, the polaron and the phonon dispersions are of the same order of magnitude and give similar bandwidths. Clear exception is in the very low density region ($r_0 = 3000$ Å), where for $d = \infty$ phonon curve has a particularly high and for $d = 20$ Å polaron curve has a particularly low value. In that density region for both $d = 20$ Å and $d = 100$ Å one finds $d/r_0 \ll 1$ which implies strong influence of the image potential[11] and therefore significant difference from the $d = \infty$ case. It explains the phonon curves, while to understand the polaron curves one has to analyze the behavior of the polaron Debye-Waller factor $S_0(\boldsymbol{\delta})$ (24). From Eqs. (19) and (9) we find $S_0(\boldsymbol{\delta}) \sim \langle W(\mathbf{k}) \rangle^2 / \omega_{\kappa p}^3$. Lower phonon frequencies (ω) are accompanied by weaker electron-electron interaction $\langle W \rangle$ so we usually obtain $S_0 < 1$ for the first neighbors. But for particularly low phonon frequencies as for $d = 20$ Å (Fig. 6), we find $S_0 > 10$, which drastically reduces the polaron bandwidth.

VI. CONCLUSION

We have analyzed the interaction of an external electron with electrons in a quasi-2D Wigner lattice on a dielectric layer with a metallic substrate, using the standard unitary transformation which incorporates the main part of the
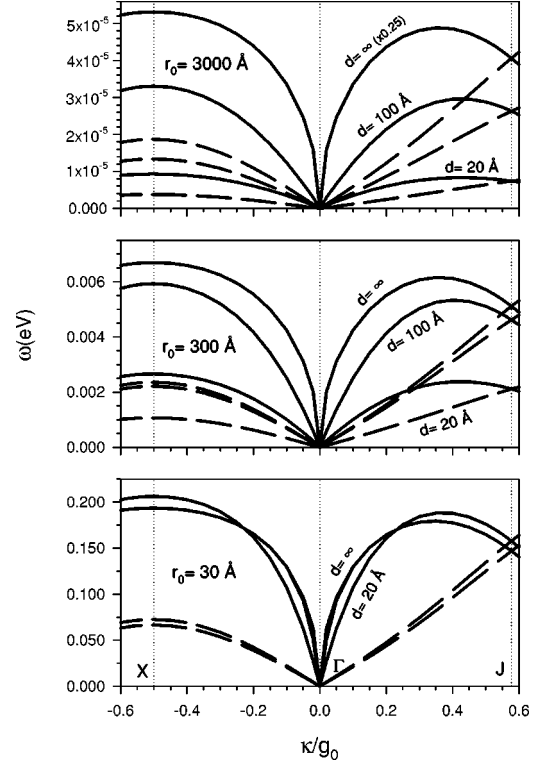

FIG. 6. Frequencies (in eV) of lattice phonons as functions of the phonon wave vector $\boldsymbol{\kappa}$ taken along the ΓX and ΓJ directions of the I BZ, in units of g_0. The curves are shown for the same d and r_0 values as in Fig. 5. The $d = \infty$ curve at $r_0 = 3000$ Å is 4 times lowered. Full lines: ω_+ mode; dashed lines: ω_- mode.

electron-phonon interaction into the diagonal part of the transformed Hamiltonian. It transforms the unperturbed phonon states into the coherent states and dresses the external electron by virtually excited phonons thus giving the polaron self-energy. The lattice is supposed to be initially in the ground state (without real phonon excitation) and we discuss the properties of a polaron in the extended small-polaron theory. We have also treated a nondiagonal part of the Hamiltonian very carefully in order to determine precisely the ground-state energy of a system as well as the polaron dispersion relation. Instead of standard tight-binding variational functions we used a complete set of Wannier functions expanded in a suitable way over the one-parameter tight-binding functions in both the direct and the Fourier spaces, so that possible corrections to the wave function can be easily added in the appropriate space. We performed the summation over the reciprocal as well as over the direct lattice vectors without any a priori restrictions, but the two parameters determining the polaron perpendicular and lateral spread show that the polaron remains well localized between lattice electrons for $r_0 > 20$ Å.

Notice that the Wannier functions were already used in the theory of Wigner lattice in order to describe regular lattice electrons.[19] In fact, in an analytical approach one has to make a decision whether to describe lattice electrons (i) by the tight-binding (Wannier) functions, using, e.g., the effective Hartree-Fock interaction, or (ii) to underline their collective behavior and treat them as phonons. In the first case one takes into account the electron exchange but ignores the correlation effects and in the second case one fully accounts

for the electron correlation but neglects electron exchange. We have adopted the second approach because for well localized lattice electrons the correlation effects are crucial. Using the Gaussian-type wave functions for lattice electrons[20] we have estimated that the exchange energy even between an external and lattice electrons can be neglected. There still remains a problem of phonon anharmonicity. It seems that these effects are not important for the Wigner lattice at $r_s > 20$,[9] but various approaches still do not give a clear answer.[4,21] Of course, all the effects can be taken into account in the first-principle numerical calculations,[9,22] but then we lack a simple physical picture.

The comparison with our previous work[5] enables us to determine the differences in the treatment of an electron-phonon interaction between the Schrödinger-Rayleigh and small-polaron approaches in this rather complicated system. According to a general rule,[10] those two approaches become closer for a larger coupling parameter. In our system the coupling is proportional to the electron-electron interaction. Since this interaction becomes weak in the presence of a strong image potential (small thickness of a dielectric layer d), we have found much better agreement between those two approaches for the electron ground-state energy in the $d \rightarrow \infty$ than in the $d = 20$ Å case.

We have found that the dispersion of the polaron energy band is strongly influenced by the image potential. When it becomes negligible, the width of the energy band is roughly proportional to the inverse of a 2D electron concentration ($\sim 1/r_0^2$), as in the case of free 2D electrons. However, the relatively large energy bandwidth is much more due to the correction of the polaron self-energy than to the corrections of the kinetic energy or a static periodic potential.

In a wide density region we have found the polaron and the lattice phonons in a similar energy range, suggesting that an external electron could become localized at a lattice site or vice versa. Within our melting theory, elaborated in detail in I, such processes define the $T = 0$ phase transition of a Wigner lattice. Following this theory we have used the calculated ground-state energy of the system to determine the critical density parameters r_c at which the phase transition occurs. At high densities we have obtained a narrow interval of critical parameters ($36 \leqslant r_c \leqslant 43$) belonging to a large interval of dielectric thicknesses (20 Å $\leqslant d \leqslant \infty$). In our previous work[8] we have applied the theory as described here to the strictly 2D Wigner lattice and obtained $r_c = 40$ in good agreement with the predicted result $r_c = 37 \pm 5$.[9] Obviously, this result gave strong support to the present work. In the low density region we have found a phase transition for $d = 20$ Å, in agreement with the simple physical consideration that a strong dipole field could destroy the Wigner lattice.[18] For $d \rightarrow \infty$ the Wigner lattice remains stable at low electron densities and at those densities ($r_s \gtrsim 1000$) it was also experimentally detected.[2]

[1] E. P. Wigner, Phys. Rev. **46**, 1002 (1934).

[2] C. C. Grimes and G. Adams, Phys. Rev. Lett. **42**, 795 (1979).

[3] L. Bonsall and A. A. Maradudin, Phys. Rev. B **15**, 1959 (1977); Z. Lenac and M. Šunjić, Phys. Rev. B **44**, 11 465 (1991).

[4] V. Tozzini and M. P. Tosi, J. Phys.: Condens. Matter **8**, 8121 (1996).

[5] Z. Lenac and M. Šunjić, Phys. Rev. B **52**, 11 238 (1995).

[6] H. Kato, F. M. Peeters, and S. E. Ulloa, Europhys. Lett. **40**, 551 (1997).

[7] A. Bianconi and M. Missori, Solid State Commun. **91**, 287 (1994).

[8] Z. Lenac and M. Šunjić, Europhys. Lett. **38**, 201 (1997).

[9] B. Tanatar and D. M. Ceperley, Phys. Rev. B **39**, 5005 (1989).

[10] See, e.g., G. D. Mahan, *Many Particle Physics* (Plenum Press, New York, 1986), Chap. 6.

[11] Z. Lenac and M. Šunjić, Phys. Rev. B **46**, 7821 (1992).

[12] S. L. Cunningham, Phys. Rev. B **10**, 4988 (1974).

[13] J. M. Kosterlitz and D. J. Thouless, J. Phys. C **6**, 1181 (1973); D. R. Nelson and B. I. Halperin, Phys. Rev. B **19**, 2457 (1979); A.

P. Young, *ibid.* **19**, 1855 (1979).

[14] S. T. Chui and K. Esferjani, Europhys. Lett. **14**, 361 (1991); B. Tanatar and S. T. Chui, J. Phys.: Condens. Matter **6**, L485 (1994); Min-Chuk Cha and H. A. Fertig, Phys. Rev. Lett. **74**, 4867 (1995).

[15] E. Cockayne and V. Elser, Phys. Rev. B **43**, 623 (1991).

[16] M. Moreno, R. M. Mendez-Moreno, and S. Orozco, J. Phys.: Condens. Matter **10**, 821 (1998).

[17] N. Choudhury and S. K. Ghosh, Phys. Rev. B **51**, 2588 (1995).

[18] F. M. Peeters and P. M. Platzman, Phys. Rev. Lett. **50**, 2021 (1983); F. M. Peeters, Phys. Rev. B **30**, 159 (1984).

[19] I. Sebasdiyar, K. Iyakutti, and M. Mahendran, Int. J. Quantum Chem. **47**, 177 (1993); K. Iyakutti and R. R. Palanichamy, *ibid.* **51**, 329 (1994).

[20] Z. Lenac and M. Šunjić, Phys. Rev. B **43**, 6049 (1991).

[21] M. C. Chang and K. Maki, Phys. Rev. B **27**, 1646 (1983); T. Kawaguchi and M. Saitoh, Solid State Commun. **88**, 765 (1993).

[22] F. G. Pikus and A. L. Efros, Solid State Commun. **92**, 485 (1994); X. Zhu and S. G. Louie, Phys. Rev. B **52**, 5863 (1995).